The application of the model mismatch strategy to improve the control performance on the example of the rotarod apparatus

Michał Awtoniuk[1]*, Miłosz Worwa[2], Robert Sałat[2],
Tomasz Makowski[2], Jędrzej Trajer[1], Kinga Sałat[3]

[1] Institute of Mechanical Engineering, Warsaw University of Life Sciences, ul. Nowoursynowska 166, 02-787 Warsaw, Poland
[2] Faculty of Electrical and Computer Engineering, Cracow University of Technology, ul. Warszawska 24, 31-155 Krakow, Poland
[3] Department of Pharmacodynamics, Chair of Pharmacodynamics, Jagiellonian University Medical College, ul. Medyczna 9, 30-688 Krakow, Poland
* Corresponding author's e-mail: michal_awtoniuk@sggw.edu.pl

ABSTRACT

The study aims to explore the application of the model mismatch strategy (MMS) to improve the speed control accuracy of a prototype rotarod apparatus (RRA), a device used to assess motor coordination in laboratory rodents. Two test scenarios were prepared: one taking into account the step change in setpoint and the other one which considered robustness to load disturbances. The control performance was assessed using integral absolute error and integral square error. The proposed MMS method significantly improved the accuracy and stability of the rotational speed control. Testing results showed control performance improvements of up to 15%. The MMS provides a novel approach to control system optimisation in preclinical research equipment, ensuring that experimental results using the RRA are more consistent and replicable.

Keywords: control, PID tuning, system identification, speed control, rotarod apparatus, motor coordination of laboratory rodents.

INTRODUCTION

The proportional-integral-derivative (PID) algorithm is widely used for the control of industrial process loops. Due to its simplicity and ease of re-tuning it remains one of the most popular control methods, even despite the passage of years [1]. According to an extensive survey carried out in the early 2000, up to 97% of control loops use the PID algorithm [2]. Among them, 64% are single loop and 36% are multi-loop. Approximately 85% of them are the feedback type, up to 6% are the feedforward type, and 9% are connected in a cascade [3].

The topics of the papers indicate the possible wide range of applications of the PID algorithm. In addition to classic applications related to motion control, chemical processes, HVAC or renewable energy, papers on medicine and pharmaceutics were also presented, e.g., drug dosing in anaesthesiology [4], blood glucose regulation. In parallel to PID systems, other control strategies are also being developed, including predictive control, adaptive control, fuzzy logic control, neural control, optimal control. However, none of these strategies has gained such a widespread use in practice as the PID algorithm [5].

Studies show that only one-third of control loops are optimally tuned [6]. Control inaccuracy is usually associated with higher material loss costs, or lower energy efficiency [2]. The tuning of a PID controller always involves an object identification process. Identification involves the determination of a parametric model describing the static and dynamic properties of the object. Depending on the process, it can be carried out

in open or closed loop, using various excitation signals, including step, pulse or harmonic signals [7]. Based on the model parameters, the controller settings are then calculated. The simplest way is to use one of the many tuning rules described in the literature; for example, O'Dwyer's study collected more than 1700 of them [8]. Another way is to use optimisation methods to find optimal settings taking into account one or more criteria, e.g. describing the quality or robustness of the control system.

The accuracy of the control will therefore depend on the accuracy of the identification. In addition, changes in the dynamics of the plant may occur over time due to ageing of materials, wear or replacement of actuators or sensors, change of operating point. These differences are referred to as model-plant mismatch [9]. In the literature, the phenomenon of model-plant mismatch is used in different ways. Sometimes studies focus on detecting differences between model and plant, e.g. to update the model [10]. Other times they use model-plant mismatch to generate artificial data to train machine learning models [11]. A description of the impact of the mismatch between model and process can most often be found in papers on MPC systems [12]. In one study [13], the effect of model mismatch on control quality is investigated, but without modifying the controller settings.

In our study, we introduced model mismatch as an additional identification step in order to assess whether this would have an effect on correcting the controller settings and consequently also on improving control performance. We called this approach the MMS. A novelty in MMS is the use of the mismatch model to re-tune the controller running in a classical feedback structure. The method was tested on a designed and built prototype of the rotarod apparatus (RRA), which is described in more detail in Section 2. The RRA is usually applied to investigate the safety profile of novel drug candidates acting on the nervous system. The MMS improves the accuracy and stability of RRA speed control. To the authors' best knowledge, in the world literature this approach applied to improve the function of this type of apparatus has not been described previously.

DESCRIPTION OF ROTAROD APPARATUS OPERATION

First described by Dunham and Miya [14], the rotarod test is one of the oldest and most widely used behavioural tests for detecting motor deficits in laboratory animals (mice and rats). Therefore, it is regarded to be of great value in preclinical research evaluating the influence of chemical compounds, including drugs and drug candidates, on motor coordination of experimental animals.

The RRA for laboratory rodents (Figure 1) is supplied with a long cylindrical rod which rotates with a forced motor activity. Several parameters can be measured using this test, such as time spent on the rotarod apparatus or endurance, and this task seems to be particularly useful for testing the effect of various drugs or assessing motor skills of experimental animals [15–17]. Because of potential concerns that the test substances will negatively influence human motor skills in the future, the rotarod test is frequently used at the early stages of drug development process to screen out chemical compounds for this potential adverse effect.

In this test, a rodent is placed on a long cylindrical rod which rotates along its long axis. When the animal falls off from the rod onto the surface below, the latency to fall (in seconds) is recorded [16]. The horizontally oriented rotating cylinder (rod) is suspended above a cage floor, which is low enough not to injure the animal, but high enough to induce avoidance of fall. Rodents naturally try to stay on the rotating cylinder, or

Figure 1. RRA available in laboratory

rotarod, and avoid falling to the ground. The length of time that a given animal stays on this rotating rod is a measure of their balance, coordination, physical condition, and motor-planning. The speed of the rotarod may either be held constant, or accelerated.

The main advantage of this test is that it very easy to perform and it gives results which can be used for statistical purposes. This test does not use subjective judgments of motor skills, and therefore its inter-rater reliability is very good. The length of time the animal stays on the rotating rod is a measure of its balance, coordination, and physical condition. Any other activity, or observations during the test, e.g., the occurrence of jumping, passive rotations can also be recorded. Moreover, these parameters may be adjusted variously to optimize the statistical separation of different conditions.

On the other hand, there are several drawbacks of this method which uses the rotarod test. Firstly, the speed of the device is mechanically driven and it can be held constant throughout the experiment, or it can be accelerated. However, if the speed is constant, some animals with poor coordination will fall off at the start of the test.

Secondly, with most devices, the researcher does not know if the speed remains the same after a load change, or if the system spins slower, or faster. Mostly, these devices use a stepper motor, and there is no feedback regarding the shaft rotation speed. This flaw can cause misinterpretation of the set shaft speed and distort final experimental results. No information is available on the implemented control algorithm and how it can be improved or adjusted.

Thirdly, inter-laboratory reliability and replicability will be achieved only if the various parameters including the size and speed of cylinder, composition material of surface, and the amount of practice/training an animal is exposed to are also thoroughly replicated.

INTRODUCTION TO MODEL MISMATCH STRATEGY

The MMS assumes the preparation of two datasets. The first dataset which can be called the learning dataset, will be used to build the initial model M_I. The second dataset, the test dataset, will be used to select a mismatched model M_M.

The first step in the MMS approach is determining the parameters of the first-order lag plus time delay (FOTD) model. This model will be treated as the initial model M_I:

$$M_I(s) = \frac{Ke^{-sL}}{Ts+1} \tag{1}$$

where: K – proportional gain, T – time constant, L – delay time.

The method of determining the M_I model parameters is arbitrary. One can use specialized software for this purpose, e.g., the system identification toolbox of the Matlab package [18], or use a classical approach, e.g., the so-called 63% step response method [19]. Regardless of the method chosen to determine the M_I model parameters, there is a risk of selecting the model with inaccuracy. The consequences of inaccuracy can have serious effects. Kula [20] showed that underestimating or overestimating the value of the time constant by 20% can increase the control settling time by 64–100%. To minimise this risk in the MMS method, we introduce a set of mismatch models based on the initial model parameters by varying the initial gain K, time constant T and delay L by the coefficients Δ_K, Δ_T and Δ_L of the assumed range:

$$M_M(s) = \frac{(\Delta_K K)e^{-s(\Delta_L L)}}{(\Delta_T T)s + 1} \tag{2}$$

where: Δ_K, Δ_T – model mismatch coefficients.

We then evaluate all models with varying coefficients Δ_K, Δ_T, and Δ_L for fit to the second dataset, i.e. the test dataset. This evaluation step is done by simulation. We determine the accuracy of the models using the NRMSE (normalized root mean square error) index, which will be abbreviated as fit:

$$fit = \left(1 - \frac{\|y(t)-\hat{y}(t)\|_2}{\|y(t)-\overline{y}\|_2}\right) \cdot 100\% \tag{3}$$

where: $y(t)$ – measured output, $\hat{y}(t)$ – simulated output, $\overline{y}$ – mean of the measured output.

The model with the highest accuracy for the test set is selected as the MM model. The controller settings are calculated according to the adopted tuning rule based on the model parameters, i.e. $\Delta_K K$, $\Delta_T T$ and $\Delta_L L$. In our research, we adopted the PI controller, described by the transfer function:

$$PI(s) = K_p \cdot \left(1 + \frac{1}{T_i s}\right) \quad (4)$$

where: K_p – controller gain, T_i – integral time.

To demonstrate the universality of the method, we chose two controller tuning rules: AMIGO [21] and SIMC [22]. The controller settings are calculated according to formulas 5 and 6 in the AMIGO and SIMC tuning rule respectively:

$$K_p = \frac{0.15}{\Delta_K K} + \left[0.35 - \frac{(\Delta_L L)(\Delta_T T)}{(\Delta_L L + \Delta_T T)^2}\right]\frac{\Delta_T T}{(\Delta_K K)(\Delta_L L)}$$
$$T_i = 0.35\Delta_L L + \frac{13(\Delta_L L)(\Delta_T T)^2}{(\Delta_T T)^2 + 12(\Delta_L L)(\Delta_T T) + 7(\Delta_L L)^2} \quad (5)$$

$$K_p = \frac{1}{\Delta_K K} \cdot \frac{\Delta_T T}{2(\Delta_L L)}$$
$$T_i = \min\{\Delta_T T, 8(\Delta_L L)\} \quad (6)$$

MATERIALS AND METHODS

Data collection scheme from the rotarod apparatus prototype

The new tuning selection method was tested on a prototype of a new generation of RRA that was constructed. The system consists of a DC motor, a rotating mass and a two-phase motor as a disturbance. The configuration also includes mechanical and control components, i.e. a power bridge to control the DC motor. The system is a single input single output (SISO) type. The system's input is the voltage [V] applied to the DC motor, and the output is the motor shaft speed (expressed as rotations per minute [rpm]). The speed is measured using

an encoder with a resolution of 400 pulses per rotation, resulting in 1 pulse per 0.9 degrees. Disturbances in the system are generated using a two-phase induction motor controlled by a voltage signal. A higher voltage means a higher load on the whole system.

Data was acquired using a computer equipped with a National Instruments NI PCIe-6323 data acquisition board using a high-speed PCI express interface, Matlab and Simulink environment (R2022b, MathWorks, Natick, MA, USA) with the desktop real-time toolbox. All signals, i.e. input u, output y and disturbance d, were acquired at 100 Hz. Figure 2 shows the block diagram of the measurement system.

Description of test scenarios

To test the effectiveness of the control performance improvement method, we performed tests assuming two scenarios: step change and load disturbance. In the first scenario, the speed setpoint y_{ref} was changed by several steps (Figure 3). In the second scenario, the setpoint was constant at one speed, and disturbances were added to the system in steps (Figure 4). The duration of the experiment in the two scenarios remained different and was 95 and 35 s fot the step change and load disturbance scenarios, respectively. We selected the value of the d and y_{ref} signals in such a way that the anti-windup mechanism would not be activated.

We conducted the tests for two sets of controller settings. The first set was calculated for the M_I model parameters, and the second one for the M_M model parameters. During the tests, we evaluated the control quality. The control quality was
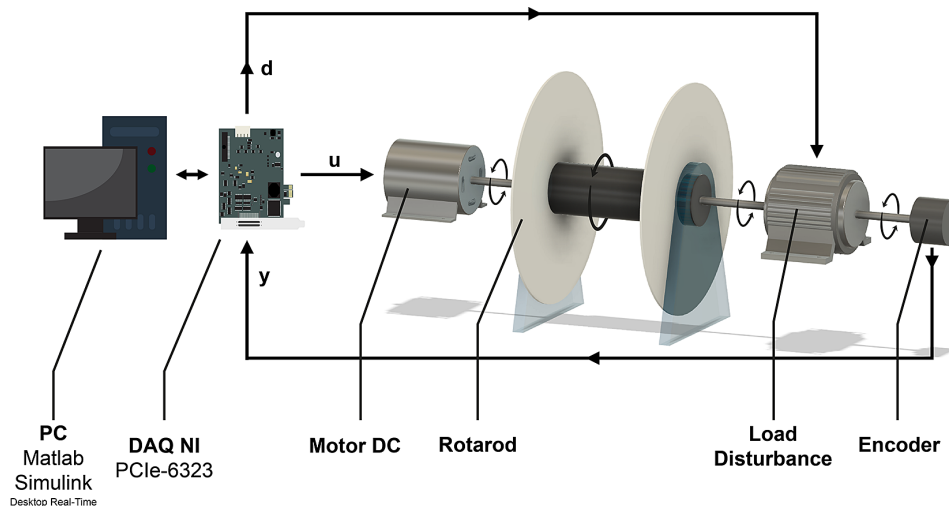

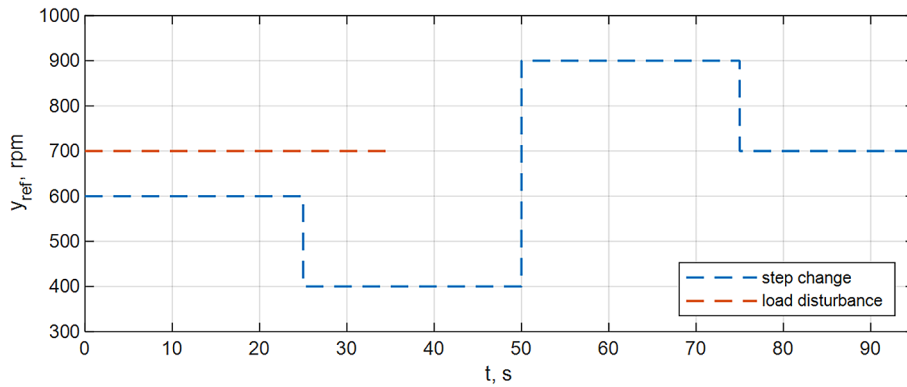**Figure 2.** Schematic of data acquisition system

Figure 3. The set point y_{ref} signal changes during step change and load disturbance test scenarios

measured using integral indices: integral absolute error (IAE) and integral square error (ISE):

$$IAE = \int |y_{ref}(t) - y(t)| dt = \sum_{t=0}^{n} |e_t| \cdot dt \quad (7)$$

$$ISE = \int [y_{ref}(t) - y(t)]^2 dt = \sum_{t=0}^{n} e_t^2 \cdot dt \quad (8)$$

where: e_t – error signal, i.e. $y_{ref}(t)$-$y(t)$, dt – sampling period, here it was equal to 0.01.

RESULTS

The learning and testing datasets are shown in Figures 5 and 6. The M_I model's parameters were determined based on the learning set. The classical 63% method determined the time constant T and the gain K. The 63% point was detected as the first sample reaching this level. The value of the delay L was also read from the step characteristics. This was the time after which the first increment of the output signal y was observed. This time can, therefore, be regarded as pure transport delay. As a result, the M_I model is described by the equation:

$$M_I(s) = \frac{Ke^{-sL}}{Ts+1} = \frac{514e^{-0.03s}}{0.48s+1} \quad (9)$$

According to the MMS assumptions, the next step was to find the M_M model by introducing the mismatch coefficients Δ_K, Δ_T and Δ_L. Since we read the transport delay time directly from the step characteristics, it is reasonable to introduce mismatch coefficients only for the gain and time constant. Based on a preliminary analysis of the impact of mismatch coefficients on model quality, we assumed the following ranges:

$$\Delta_K \in \{0.8, 0.84, 0.88, \dots, 1.12, 1.16, 1.2\}$$
$$\Delta_T \in \{0.2, 0.36, 0.52, \dots, 1.48, 1.64, 1.8\} \quad (10)$$
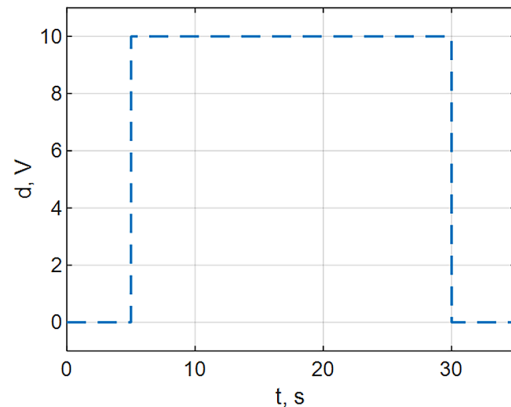$$\Delta_L = 1$$

Figure 4. The disturbance d signal changes during load disturbance test scenario

During the simulation study, the entire set of resulting models was assessed for fit to the test set. Figure 7 shows the fit index values obtained during this study. The model with the highest index value (red dot in Figure 7) was selected as the M_M model. Thus, the mismatch coefficients of the M_M model are $\Delta_K = 1$ and $\Delta_T = 1.64$, respectively.

The M_M model is described by the transfer function (11). A comparison of the Fit coefficients of the two models is shown in Table 1.

$$M_M(s) = \frac{(\Delta_K K)e^{-s(\Delta_L L)}}{(\Delta_T T)s + 1} = \frac{514e^{-0.03s}}{0.787s + 1} \quad (11)$$

To evaluate the effectiveness of the MMS, we chose two tuning rules: AMIGO and SIMC. These

Table 1. Calculated model quality metrics

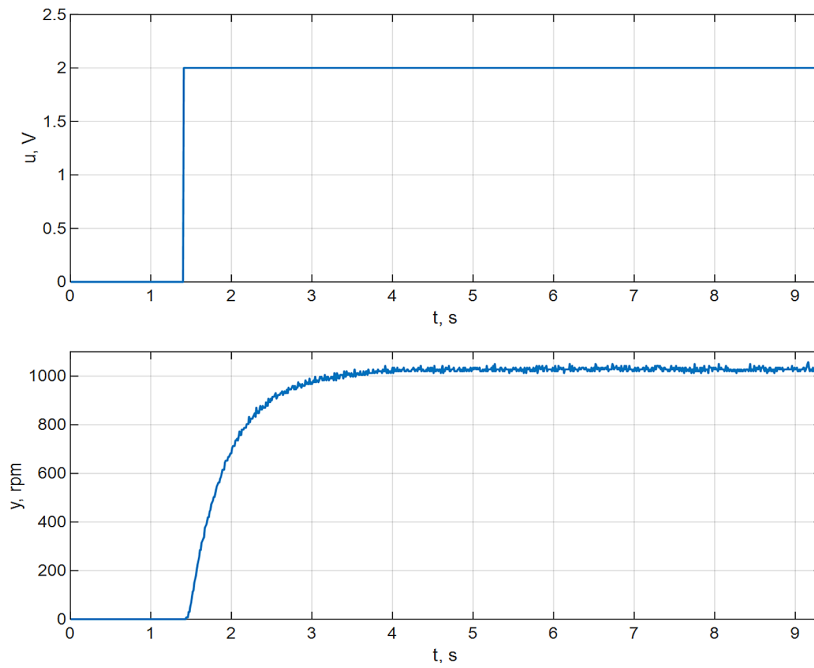| Model	Fit [%]	
	Learning dataset	Testing dataset
M_I	97.14	77.83
M_M	84.65	80.34

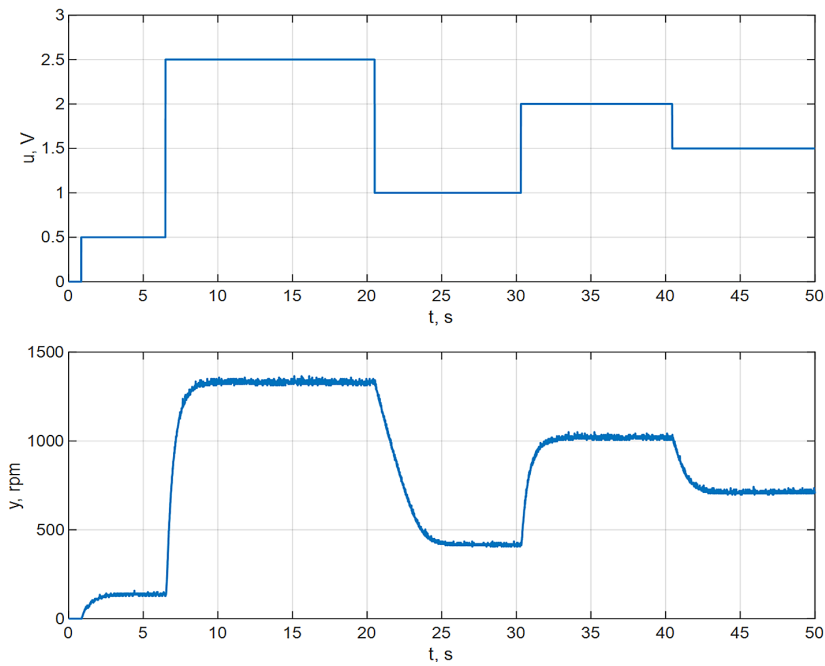**Figure 5.** Input u and output signal y in the learning dataset

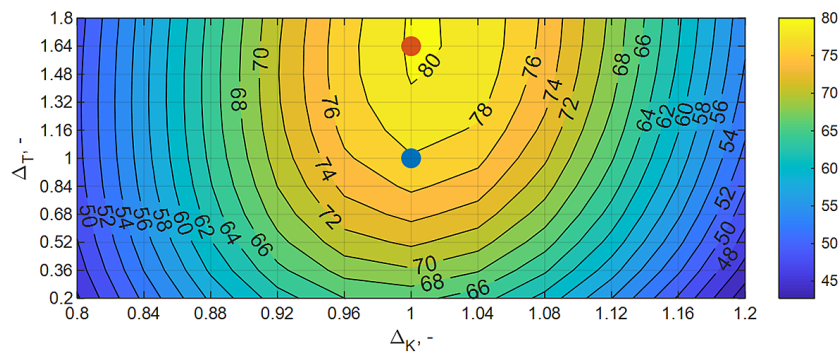**Figure 6.** Input u and output signal y in the testing dataset

Figure 7. Fit index for the testing dataset with different values of the mismatch model parameters: blue dot indicates the M_I model, red dot indicates the model with the highest fit, i.e. the selected M_M model

rules were also tested by Hägglund [6]. The PI controller parameters calculated for each method based on the M_I and M_M models are shown in Table 2. The calculated controller settings were tested in two test scenarios. The test runs with settings according to the AMIGO rule are shown in Figures 8 (for the step change scenario) and 9 (for the load disturbance scenario). Similarly, Figures 10 and 11 show the test runs for the SIMC rule. The results of the experiments summarized in the form of IAE and ISE quality index values are presented in Table 3.

Table 2. Calculated controller parameters

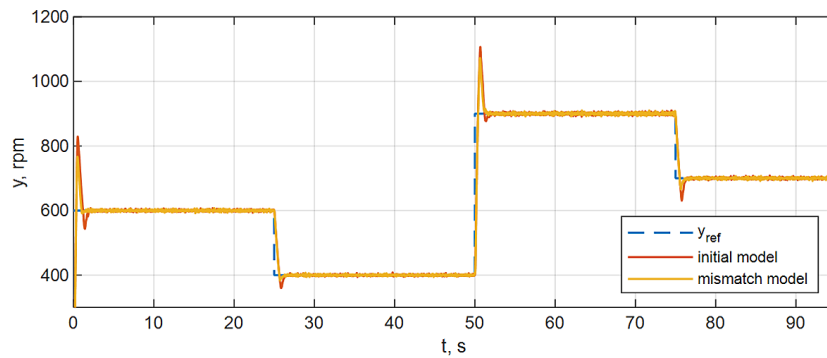| Model	K_p [-]	T_i [s]
AMIGO tuning rule		
M_I	0.0095	0.2299
M_M	0.0164	0.2763
SIMC tuning rule		
M_I	0.0156	0.24
M_M	0.0255	0.24

Figure 8. Plant output y for AMIGO tuning rule in step change scenario
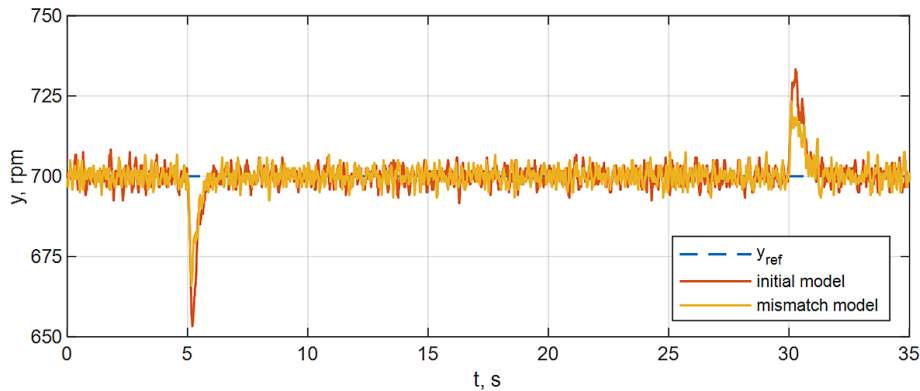

Figure 9. Plant output y for AMIGO tuning rule in load disturbance scenario

Table 3. Control performance assessed for M_I and M_M models

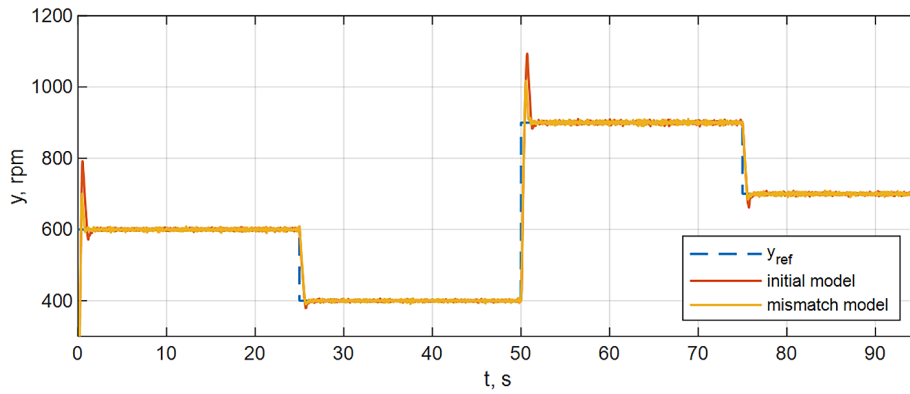| Model	Step change		Load disturbance	
	IAE [-]	ISE [-]	IAE [-]	ISE [-]
AMIGO tuning rule				
M_I	748	$1.35 \cdot 10^5$	92.5	1 009
M_M	644	$1.22 \cdot 10^5$	84.1	567
SIMC tuning rule				
M_I	674	$1.30 \cdot 10^5$	78	532
M_M	573	$1.10 \cdot 10^5$	80.9	374

Figure 10. Plant output y for SIMC tuning rule in step change scenario
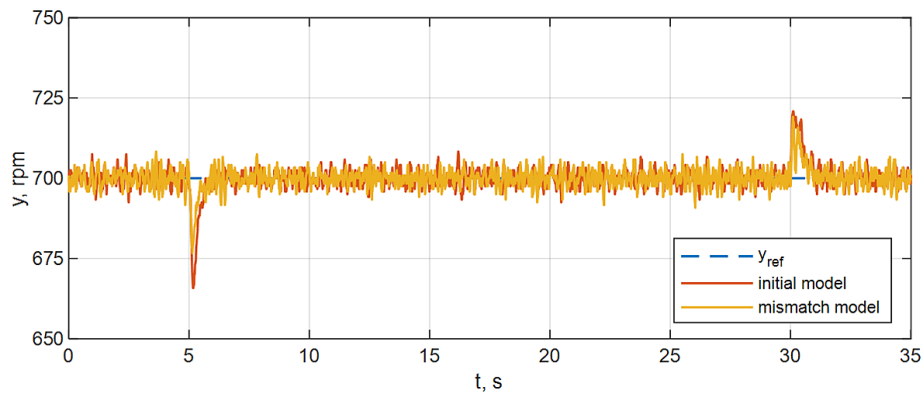

Figure 11. Plant output y for SIMC tuning rule in load disturbance scenario

DISCUSSION

For the AMIGO tuning rule, applying the MMS increased the value of the gain K_p by approximately 73% (from 0.0095 to 0.0164). It increased the integration time T_i by approximately 20% (from 0.2299 s to 0.2763 s). For the SIMC tuning rule, a similar pattern was observed for the K_p value, i.e. an increase of approximately 64% (from 0.0156 to 0.0255). In contrast, the integration time T_i remained unchanged (0.24 s). This follows directly from the formulae (6). The mismatch model parameters only changed concerning the time constant T ($\Delta_T = 1.64, \Delta_K = 1, \Delta_L = 1$). The control objects the FOTD model can describe are categorized into three groups: lag-dominated, balanced or delay-dominated. Belonging to a category is determined by the value of the normalized time delay τ calculated as:

$$\tau = \frac{L}{L + T} \qquad (12)$$

The literature conventionally indicates the following ranges for each category: $0 \leq \tau \leq 0.2$ for lag-dominated, $0.2 < \tau < 0.6$ for balanced and $0.6 \leq \tau \leq 1$ for delay-dominated processes [6,7,23]. The M_I and M_M models' normalized time delay values were 0.059 and 0.037. In both cases, it was lag-dominated object dynamics. According to a detailed analysis [6], in AMIGO and SIMC, the gain K_p has the highest values and the most significant variability for lag-dominated objects. This may be a suggestion for matching the tuning rule to the model dynamics. Tuning rules that show more significant variability of the controller parameters with a change in the model dynamics will have a chance for a more remarkable improvement in the control quality when using MMS.

Testing of the step-change setpoint scenario showed that the use of MMS led to an improvement in control performance for both tuning rules (AMIGO and SIMC). The IAE and ISE indices were reduced, meaning the desired speed was maintained more accurately with step changes. A reduction of about 14% in the IAE index (from 748 to 644) and about 10% in the ISE index (from $1.35 \cdot 10^5$ to $1.22 \cdot 10^5$) was achieved. In the case of the SIMC rule, the values of both indices

17

decreased by about 15% (from 674 to 573 for IAE and from $1.30 \cdot 10^5$ to $1.10 \cdot 10^5$ for ISE).

For the load disturbance scenario, the results are more varied. For the AMIGO rule, MMS benefited both indices – IAE decreased by more than 9% (from 92.5 to 84.1) and ISE by nearly 44% (from 1009 to 567). In contrast, for the SIMC rule, the IAE index increased by less than 4% (from 78 to 80.9). At the same time, the ISE index improved significantly, decreasing by almost 30% (from 532 to 374). The differences in the IAE index for the SIMC rule are due to the integration intensity of the controller. In both cases, the parameter T_i was the same (0.24 s), but as can be seen from the transfer function of the controller (4), the integration action is also affected by the value of the gain K_p. Finally, the integration action of the controller calculated according to the M_I model parameters is more intensive. This results in a slightly more effective minimisation of the control error. An increase in the IAE index with a simultaneous decrease in the ISE may indicate that errors of smaller amplitude but with a greater frequency are occurring in the system. The controller reacts more quickly, oscillating the controlled signal with a small amplitude. The benefit of this case is that more significant errors caused by a sudden spike in disturbances will be compensated more quickly. In the load disturbance scenario, this behaviour was desirable.

CONCLUSIONS

The results of the present study lead to the following conclusions:

- the use of MMS appeared to be an effective way to improve the control performance of the RRA, which is an example of a lag-dominated control object. We observed an improvement in control performance regardless of the chosen tuning rule,
- the effect of MMS on control performance of the RRA was particularly beneficial for step changes in the setpoint. The performance indices were reduced irrespective of the adopted tuning rule,
- in the case of a load disturbance scenario, using MMS significantly improved the reduction of significant amplitude errors,
- using a control based on a PID algorithm in the RRA prototype provides confidence that the speed set by the operator will be precisely

maintained, which is not guaranteed in the currently available rotarod devices.

The MMS was used to improve the function of the RRA. At present, this might be regarded as a potential limitation of the present study because the method proposed was tested with the use of only one type of devices used for behavioural pharmacological testing. It has to be noted therefore that we are planning to develop the MMS further. In our future work, we intend to apply MMS to balanced and delay-dominated control systems. We will also attempt to evaluate the method with the active use of the Δ_L coefficient, modifying the transport delay of the model.

REFERENCES

1. Åström K J and Hägglund T. The future of PID control. Control Engineering Practice 2001; 9 1163–75.

2. Desborough L and Miller R. Increasing Customer value of industrial control performance monitoring -honeywell's experience. AIChE Symposium Series 2002; 98.

3. Li Y, Ang K H and Chong G C Y. Patents, software, and hardware for PID control: an overview and analysis of the current art IEEE Control Systems Magazine 2006; 26: 42–54.

4. Pawlowski A, Schiavo M and Visioli A. A PID-based structure for MISO approach to anaesthesia control problem. IFAC-PapersOnLine 2024; 58: 240–5.

5. Hägglund T and Guzmán J L. Give us PID controllers and we can control the world IFAC-PapersOnLine 2024; 58: 103–8.

6. Hägglund T. The one-third rule for PI controller tuning. Computers & Chemical Engineering 2019; 127: 25–30.

7. Awtoniuk M, Sałat R, Worwa M and Reshetiuk V. Implementation of PID autotuning procedure based on doublet-pulse method in PLC controller Adv. Sci. Technol. Res. J. 2024; 18: 89–97.

8. O'Dwyer A. Handbook of PI and PID Controller Tuning Rules 2009. (published by imperial college press and distributed by world scientific publishing co.)

9. Botelho V R, Trierweiler J O, Farenzena M and Duraiski R. Assessment of model-plant mismatch by the nominal sensitivity function for unconstrained

MPC. IFAC-PapersOnLine 2015; 48: 753–8.

10. Shi Y, Yuan Y, Luo B, Li F, Xu X and Yang C. Data-driven plant–model mismatch detection for closed-loop LPV system based on instrumental variable using sum-of-norms regularization. IEEE Transactions on Instrumentation and Measurement 2024; 73: 1–12.

11. Lu Y, Huang K, Wang B, Lai C and Feng G. Data-driven modeling and compensation strategy of PMSM considering core loss and saturation. IEEE Journal of Emerging and Selected Topics in Power Electronics 2024; 12: 1894–905.

12. Shende D R and Simon A. Implementation and performance evaluation of a model predictive controller for a semi-autogenous grinding mill. Adv. Sci. Technol. Res. J. 2024; 18: 257–69.

13. Tufa L D and Ka C Z. Effect of model plant mismatch on MPC performance and mismatch threshold determination. Procedia Engineering 2016; 148: 1008–14.

14. Dunham N W and Miya T S. A note on a simple apparatus for detecting neurological deficit in rats and mice. J Am Pharm Assoc Am Pharm Assoc 1957; 46: 208–9.

15. Sałat K, Furgała A and Sałat R. Interventional and preventive effects of aripiprazole and ceftriaxone used alone or in combination on oxaliplatin-induced tactile and cold allodynia in mice. Biomedicine & Pharmacotherapy 2019; 111: 882–90.

16. Sałat K, Gawlik K, Witalis J, Pawlica-Gosiewska D, Filipek B, Solnica B, Więckowski K and Malawska B. Evaluation of antinociceptive and antioxidant properties of 3-[4-(3-trifluoromethyl-phenyl)-piperazin-1-yl]-dihydrofuran-2-one in mice. Naunyn-Schmiedeberg's Archives of Pharmacology 2013; 386: 493.

17. Knez D, Diez-Iriepa D, Chioua M, Gottinger A, Denic M, Chantegreil F, Nachon F, Brazzolotto X, Skrzypczak-Wiercioch A, Meden A, Pišlar A, Kos J, Žakelj S, Stojan J, Sałat K, Serrano J, Fernández A P, Sánchez-García A, Martínez-Murillo R, Binda C, López-Muñoz F, Gobec S and Marco-Contelles J. 8-Hydroxyquinolylnitrones as multifunctional ligands for the therapy of neurodegenerative diseases. Acta Pharmaceutica Sinica B 2023; 13: 2152–75.

18. Tangirala A K. Principles of system identification : theory and practice (Boca Raton: CRC Press) 2015.

19. Cohen G H and Coon G A. Theoretical consideration of retarded control. Journal of Fluids Engineering 1953; 75: 827–34

20. Kula K S. Tuning a PI/PID controller with direct synthesis to obtain a non-oscillatory response of time-delayed systems. Applied Sciences 2024; 14: 5468.

21. Aström K J and Hägglund T. Advanced PID Control (Research Triangle Park, NC: International Society of Automation) 2005.

22. Skogestad S. Simple analytic rules for model reduction and PID controller tuning Journal of Process Control 2003; 13: 291–309.

23. Berner J, Hägglund T and Åström K J. Asymmetric relay autotuning – Practical features for industrial use. Control Engineering Practice 2016; 54: 231–45.